The Direct Synthesis of Hydrogen Peroxide over AuPd Nanoparticles: An Investigation into Metal Loading

Joseph Brehm[1] · Richard J. Lewis[1] · David J. Morgan[1,2] · Thomas E. Davies[1] · Graham J. Hutchings[1]

Abstract

The direct synthesis of H_2O_2 from molecular H_2 and O_2 over AuPd catalysts, supported on TiO_2 and prepared via an excess chloride co-impregnation procedure is investigated. The role of Au:Pd ratio on the catalytic activity towards H_2O_2 formation and its subsequent degradation is evaluated under conditions that have previously been found to be optimal for the formation of H_2O_2. The combination of relatively small nanoparticles, of mixed Pd-oxidation state is shown to correlate with enhanced catalytic performance. Subsequently, a detailed study of catalytic activity towards H_2O_2 synthesis as a function of AuPd loading was conducted, with a direct correlation between catalytic activity and metal loading observed.

Graphic Abstract
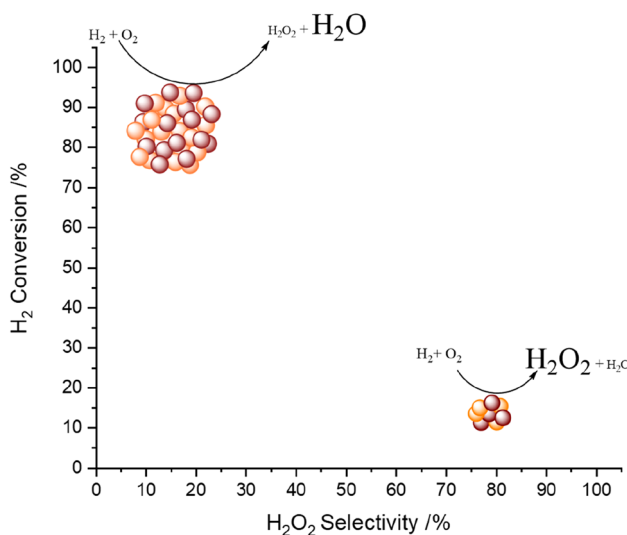
Joseph Brehm and Richard J. Lewis contributed equally to this work.

✉ Richard J. Lewis
    LewisR27@Cardiff.ac.uk

✉ Graham J. Hutchings
    Hutch@Cardiff.ac.uk

1   School of Chemistry, Cardiff University, Main Building, Park Place, Cardiff CF10 3AT, UK

2   HarwellXPS, Research Complex at Harwell (RCaH), Didcot OX11 OFA, UK

1 Introduction

Hydrogen peroxide (H_2O_2) is a powerful, environmentally friendly oxidant with an active oxygen content second only to molecular oxygen. Finding major application in industries where its efficacy as a bleaching agent is required or those that rely on its high active oxygen potential, such as in the chemical synthesis sector, H_2O_2 is considered a green alternative to traditional stoichiometric oxidants, such as sodium

hypochlorite or permanganate, with only water resulting from its application [1].

The direct synthesis of H_2O_2 from molecular H_2 and O_2 would offer an attractive on-site alternative to the current industrial means of H_2O_2 production, the anthraquinone oxidation (AO) process. Due to economies of scale H_2O_2 production via the AO process is typically centralized, with H_2O_2 often shipped at concentrations far higher than those required by the end user. As such a significant amount of energy, associated with the distillation and concentration of H_2O_2 to such high concentrations, prior to shipping is effectively wasted [2, 3]. Furthermore, the relative instability of H_2O_2, readily decomposing to water in the presence of mild temperatures or weak bases typically necessitates the use of stabilizing agents, with phosphoric acid [4], acetic acid [5] and quinolic acid [6] often used. Finally, there are concerns associated with the carbon-efficiency of the AO process, with the over hydrogenation of the anthraquinone carrier molecule necessitating its periodic replacement. As such an alternative means to produce H_2O_2 on-site, at desirable concentrations would have major economic and environmental benefits and to this end the direct synthesis of H_2O_2 from molecular H_2 and O_2, has been extensively studied [1, 3, 7–9].

While Pd-based catalysts have been well reported to offer high activity towards H_2O_2 production via the direct route [1, 3, 10–14], there has been extensive investigation into the alloying of Pd with secondary metals to improve catalytic performance [15–24]. Indeed, the introduction of Au into supported Pd catalysts has been widely demonstrated to improve catalytic efficacy, with electronic, structural and isolation effects all potential causes for the enhanced performance typically observed in AuPd bi-metallic systems [25–28]. Indeed we have previously reported the ability of Au to promote the catalytic performance of Pd-based catalysts over a range of reaction conditions [28]. There is general agreement that the enhanced catalytic selectivity observed as a result of AuPd alloying originates, in-part, from the ability of Au to inhibit O–O bond scission, and the resulting formation of H_2O. Indeed, several studies have reported that in comparison to Pd-only analogues, AuPd surfaces interact less strongly with H_2O_2, with the energetic favourability of O–O bond cleavage of Pd surfaces greatly reduced through the introduction of Au [29–31].

With these earlier studies in mind and with growing interest in the continual supply of low concentrations of H_2O_2 to facilitate chemical transformations [32] we now investigate the effect of metal loading on the ability of AuPd catalysts on the direct synthesis of H_2O_2.

2 Experimental

2.1 Catalyst Preparation

Mono- and bi-metallic $AuPd/TiO_2$ catalysts have been prepared (on a weight basis) by an excess chloride co-impregnation procedure, based on a methodology previously reported in the literature, which has been shown to improve dispersion of metal species, particularly Au [33]. The procedure to produce 0.5% Au–0.5% Pd/TiO_2 (2 g) is outlined below, with a similar methodology utilized for all catalysts.

Aqueous acidified $PdCl_2$ solution (1.667 mL, 0.58 M HCl, 6 mg mL^{-1}, Merck) and aqueous $HAuCl_4 \cdot 3H_2O$ solution (0.8263 mL, 12.25 mg mL^{-1}, Strem Chemicals) were mixed in a 50 mL round-bottom flask and heated to 65 °C with stirring (1000 rpm) in a thermostatically controlled oil bath, with total volume fixed to 16 mL using H_2O (HPLC grade, Fischer Scientific). Upon reaching 65 °C, TiO_2 (1.98 g, Degussa, P25) was added over the course of 5 min with constant stirring. The resulting slurry was stirred at 65 °C for a further 15 min, following this the temperature was raised to 95 °C for 16 h to allow for complete evaporation of water. The resulting solid was ground prior to a reductive heat treatment (5% H_2/Ar, 400 °C, 4 h, 10 °C min^{-1}). Alternatively, selected samples were subjected to an oxidative heat treatment (flowing air, 400 C, 3 h, 10 °C min^{-1}), with additional samples exposed to a reductive heat treatment (5% H_2/Ar, 200–400 °C, 4 h, 10 °C min^{-1}).

Surface area measurements of 0.5% Au–0.5% Pd/TiO_2 and monometallic Au and Pd analogues as determined by 5-point N_2 adsorption, are reported in Table S.1.

2.2 Catalyst Testing

2.2.1 Note 1

Reaction conditions used within this study operate below the flammability limits of gaseous mixtures of H_2 and O_2.

2.2.2 Note 2

The conditions used within this work for H_2O_2 synthesis and degradation have previously been investigated, with the presence of CO_2 as a diluent for reactant gases and a methanol co-solvent identified as key to maintaining high catalytic efficacy towards H_2O_2 production [28, 34].

2.2.2.1 Direct Synthesis of H_2O_2 from H_2 and O_2 Hydrogen peroxide synthesis was evaluated using a Parr Instruments stainless steel autoclave with a nominal volume of 100 mL, equipped with a PTFE liner and a maximum working pres-

sure of 2000 psi. To test each catalyst for H_2O_2 synthesis, the autoclave liner was charged with catalyst (0.01 g) and HPLC standard solvents (5.6 g methanol and 2.9 g H_2O, both Fischer Scientific). The charged autoclave was then purged three times with 5% H_2/CO_2 (100 psi) before filling with 5% H_2/CO_2 to a pressure of 420 psi, followed by the addition of 25% O_2/CO_2 (160 psi). Pressure of 5% H_2/CO_2 and 25% O_2/CO_2 are given as gauge pressures and reactant gasses are not continually supplied. The reaction was conducted at a temperature of 2 °C, for 0.5 h with stirring (1200 rpm), with the reactor temperature controlled using a HAAKE K50 bath/circulator using an appropriate coolant.

H_2O_2 productivity was determined by titrating aliquots of the final solution after reaction with acidified $Ce(SO_4)_2$ (0.0085 M) in the presence of ferroin indicator. Catalyst productivities are reported as $mol_{H2O2} \, kg_{cat}^{-1} \, h^{-1}$.

Total autoclave capacity was determined via water displacement to allow for accurate determination of H_2 conversion and H_2O_2 selectivity. When equipped with a PTFE liner, the total volume of an unfilled autoclave was determined to be 93 mL, which includes all available gaseous space within the autoclave.

Catalytic conversion of H_2 and selectivity towards H_2O_2 were determined using a Varian 3800 GC fitted with TCD and equipped with a Porapak Q column.

H_2 conversion (Eq. 1) H_2O_2 selectivity (Eq. 2) are defined as follows:

$$H_2 \text{Conversion} (\%) = \frac{mmol_{H2(t(0))} - mmol_{H2(t(1))}}{mmol_{H2(t(0))}} \times 100 \tag{1}$$

$$H_2O_2 \text{ Selectivity} (\%) = \frac{H_2O_2 \text{detected (mmol)}}{H_2 \text{ consumed (mmol)}} \times 100 \tag{2}$$

2.2.2.2 Degradation of H_2O_2 Catalytic activity towards H_2O_2 degradation (via hydrogenation and decomposition pathways) was determined in a similar manner to that used to measure the direct synthesis activity of a catalyst. The autoclave liner was charged with methanol (5.6 g, HPLC standard, Fischer Scientific), H_2O_2 (50 wt.%, 0.69 g, Merck), H_2O (2.21 g, HPLC standard, Fischer Scientific) and catalyst (0.01 g), with the solvent composition equivalent to a 4 wt.% H_2O_2 solution. From the solution, prior to the addition of the catalyst, two 0.05 g aliquots were removed and titrated with acidified $Ce(SO_4)_2$ solution using ferroin as an indicator to determine an accurate concentration of H_2O_2 at the start of the reaction. The autoclave was purged three times with 5% H_2/CO_2 (100 psi) before filling with 5% H_2/CO_2 to a gauge pressure of 420 psi. The reaction was conducted at a temperature of 2 °C, for 0.5 h with stirring (1200 rpm). After the reaction was complete the catalyst was removed from the reaction mixture by filtration and two

0.05 g aliquots were titrated against the acidified $Ce(SO_4)_2$ solution using ferroin as an indicator. The degradation activity is reported as $mol_{H2O2} \, kg_{cat}^{-1} \, h^{-1}$.

2.2.2.3 Time-on-Line Analysis for the Direct Synthesis of H_2O_2 An identical procedure to that outlined above for the direct synthesis of H_2O_2 is followed for the desired reaction time. It should be noted that individual experiments are carried out and the reaction mixture is not sampled on-line.

2.2.2.4 Gas Replacement Experiments for the Direct Synthesis of H_2O_2 An identical procedure to that outlined above for the direct synthesis of H_2O_2 was followed for a reaction time of 0.5 h. After this, stirring was stopped and the reactant gas mixture was vented prior to replacement with the standard pressures of 5% H_2/CO_2 (420 psi) and 25% O_2/CO_2 (160 psi). The reaction mixture was then stirred (1200 rpm) for a further 0.5 h. To collect a series of data points, as in the case of Fig. 2, it should be noted that individual experiments were carried out and the reactant mixture was not sampled on-line.

2.2.2.5 Catalyst Reusability in the Direct Synthesis and Degradation of H_2O_2 In order to determine catalyst reusability a similar procedure to that outlined above for the direct synthesis of H_2O_2 is followed utilising 0.05 g of catalyst. Following the initial test, the catalyst is recovered by filtration and dried (30 °C, 16 h, under vacuum), from the recovered catalyst sample 0.01 g is used to conduct a standard H_2O_2 synthesis or degradation experiment.

2.2.2.6 The Effect of Cl^- as a Promoter in the Direct Synthesis of H_2O_2 In order to determine the promotive effect of Cl^- on catalytic activity towards H_2O_2 an identical procedure to that outlined above for the direct synthesis of H_2O_2 was followed utilising 0.05 g of catalyst. Following the initial test, the catalyst is recovered by filtration and dried (30 °C, 16 h, under vacuum), from the recovered catalyst sample 0.01 g is used to conduct a standard H_2O_2 synthesis, where a proportion of the water co-solvent is replaced with aqueous Cl in the form of $MgCl_2$ or $CaCl_2$ at concentrations of Cl comparable to that present in the fresh catalyst.

2.2.2.7 Catalyst Characterisation Brunauer Emmett Teller (BET) surface area measurements were conducted using a Quadrasorb surface area analyser. A 5-point isotherm of each material was measured using N_2 as the adsorbate gas. Samples were degassed at 250 °C for 2 h prior to the surface area being determined by 5-point N_2 adsorption at −196 °C, and data analysed using the BET method.

A Thermo Scientific K-Alpha$^+$ photoelectron spectrometer was used to collect XP spectra utilising a micro-focused monochromatic Al K_α X-ray source operating at 72 W.

Data was collected over an elliptical area of approximately 400 μm^2 at pass energies of 40 and 150 eV for high-resolution and survey spectra, respectively. Sample charging effects were minimised through a combination of low energy electrons and Ar$^+$ ions, consequently this resulted in a C(1 s) line at 284.8 eV for all samples. All data was processed using CasaXPS v2.3.24 using a Shirley background, Scofield sensitivity factors [35] and an electron energy dependence of − 0.6 as recommended by the manufacturer.

The bulk structure of the catalysts was determined by powder X-ray diffraction using a (θ–θ) PANalytical X'pert Pro powder diffractometer using a Cu K$_\alpha$ radiation source, operating at 40 keV and 40 mA. Standard analysis was carried out using a 40 min run with a back filled sample, between 2θ values of 10–80°. Phase identification was carried out using the International Centre for Diffraction Data (ICDD).

Transmission electron microscopy (TEM) was performed on a JEOL JEM-2100 operating at 200 kV. Samples were prepared by dispersion in ethanol by sonication and deposited on 300 mesh copper grids coated with holey carbon film. Energy dispersive X-ray analysis (EDX) was performed using an Oxford Instruments X-Max^N 80 detector and the data analysed using the Aztec software.

Total metal leaching from the supported catalyst was quantified via inductively coupled plasma mass spectrometry (ICP-MS). Post-reaction solutions were analysed using an Agilent 7900 ICP-MS equipped with I-AS auto-sampler. All samples were diluted by a factor of 10 using HPLC grade H$_2$O (1% HNO$_3$ and 0.5% HCl matrix). All calibrants were matrix matched and measured against a five-point calibration using certified reference materials purchased from Perkin Elmer and certified internal standards acquired from Agilent.

3 Results and Discussion

In keeping with numerous previous works [29, 36], our initial studies established the ability of Au incorporation into a supported Pd catalyst to significantly improve catalytic performance towards H$_2$O$_2$ synthesis, with H$_2$O$_2$ formation rates over the 0.5% Au–0.5% Pd/TiO$_2$ catalyst (96 mol$_{H2O2}$ kg$_{cat}^{-1}$ h^{-1}) far greater than that observed over the analogous Au- (1 mol$_{H2O2}$ kg$_{cat}^{-1}$ h^{-1}) or Pd-only (26 mol$_{H2O2}$ kg$_{cat}^{-1}$ h^{-1}) materials (Table 1). A corresponding decrease in H$_2$O$_2$ degradation (via hydrogenation and decomposition) is also observed upon Au introduction, with the activity of the 1% Pd/TiO$_2$ catalyst (269 mol$_{H2O2}$ kg$_{cat}^{-1}$ h^{-1}) somewhat greater than that of the 0.5% Au–0.5% Pd/TiO$_2$ catalyst (227 mol$_{H2O2}$ kg$_{cat}^{-1}$ h^{-1}).

Analysis of the 1% AuPd/TiO$_2$ catalysts, reported in Table 1, by X-ray diffraction (Figure S.1) reveals no reflections associated with either Au or Pd, likely resulting from

Table 1 Catalytic activity towards the direct synthesis and subsequent degradation of H$_2$O$_2$

Catalyst	Productivity/ mol$_{H2O2}$ kg$_{cat}^{-1}$ h^{-1} (H$_2$O$_2$ wt.%)	Degradation/ mol$_{H2O2}$ kg$_{cat}^{-1}$ h^{-1}
1%Au/TiO$_2$	1 (0.003)	9
0.75% Au–0.25% Pd/ TiO$_2$	32 (0.070)	70
0.5% Au–0.5% Pd/TiO$_2$	96 (0.190)	227
0.25% Au–0.75% Pd/ TiO$_2$	87 (0.180)	247
1% Pd/TiO$_2$	26 (0.050)	269

H$_2$O$_2$ direct synthesis reaction conditions: Catalyst (0.01 g), H$_2$O (2.9 g), MeOH (5.6 g), 5% H$_2$/CO$_2$ (420 psi), 25% O$_2$/CO$_2$ (160 psi), 0.5 h, 2 °C 1200 rpm. H$_2$O$_2$ degradation reaction conditions: Catalyst (0.01 g), H$_2$O$_2$ (50 wt.% 0.68 g) H$_2$O (2.22 g), MeOH (5.6 g), 5% H$_2$/CO$_2$ (420 psi), 0.5 h, 2 °C 1200 rpm

Table 2 Mean particle size of 1% AuPd/TiO$_2$ catalysts, prepared via an excess chloride impregnation methodology, as determined by transmission electron microscopy

Catalyst	Mean particle size/ nm (Standard deviation)
1% Au/TiO$_2$	24.9 (7.9)
0.75% Au–0.25% Pd/TiO$_2$	13.1 (8.3)
0.5% Au–0.5% Pd/TiO$_2$	4.2 (1.8)
0.25% Au–0.75% Pd/TiO$_2$	6.5 (8.5)
1% Pd/TiO$_2$	n.d*

*Unable to determine due to particle sizes being below TEM limits of detection

the low total metal loading of these materials. While measurement of the mean nanoparticle size (Table 2) as determined by bright field transmission electron microscopy (BF-TEM) (representative micrographs can be seen in Figure S.2) indicates that upon the alloying of Au and Pd, mean particle size decreases dramatically compared to the 1% Au/TiO$_2$ catalyst (24.9 nm), with the 0.5% Au–0.5% Pd/TiO$_2$ catalyst displaying a mean particle size of 4.2 nm. Although it is interesting to note that the mean particle size of the 0.25% Au–0.75% Pd/TiO$_2$ catalyst is somewhat larger than that of both the 0.5% Au–0.5% Pd/TiO$_2$ and 1% Pd/TiO$_2$ analogues, indicating that Au: Pd ratio can have a significant effect on metal dispersion. Further analysis via X-ray photoelectron spectroscopy (XPS) (Figure S.3) reveals that the introduction of Au into a monometallic Pd catalyst significantly modifies Pd-oxidation state, with an increase in Pd^{2+} content observed. The presence of domains of mixed Pd oxidation state has been well reported to improve catalytic performance towards H$_2$O$_2$ synthesis compared to Pd^{2+} or Pd^0-rich analogues [37–39]. As such, we consider that

this combination of relatively small nanoparticles, of mixed Pd-oxidation state may be a key factor responsible for the enhanced activity observed over the 0.5% Au–0.5% Pd/TiO$_2$ catalyst.

For numerous applications, the continual in-situ production of low concentrations of stabiliser free H$_2$O$_2$ would be preferred, compared to the addition of aqueous solutions of H$_2$O$_2$ [32]. With this in mind and building on our initial studies, we subsequently established the activity of a series of supported AuPd catalysts, of various total metal loading, toward the direct synthesis of H$_2$O$_2$ (Table 3). A direct relationship between total nominal metal loading and catalytic activity towards both H$_2$O$_2$ synthesis and its subsequent degradation is apparent, with the 0.5% Au–0.5% Pd/TiO$_2$ catalyst offering the greatest activity towards both reaction pathways. Interestingly the 0.0625% Au–0.0625% Pd/TiO$_2$ catalyst offers exceptionally low activity towards H$_2$O$_2$ synthesis, possibly lower than would be expected given the strong correlation between metal content and catalytic performance observed across the catalyst series. In keeping with the observed correlation between total metal loading and H$_2$O$_2$ degradation, catalytic selectivity towards H$_2$ (i.e. the amount of H$_2$ utilised in the production of H$_2$O$_2$) is also seen to correlate well with metal content, with the 0.125% Au–0.125% Pd/TiO$_2$ catalyst displaying higher selectivity towards H$_2$ (71%), that higher metal loading analogues.

With the observed variation in catalytic performance under our standard reaction conditions, we were motivated to further investigate this series of supported AuPd catalysts. Time-on-line studies comparing catalytic performance towards H$_2$O$_2$ production over the supported AuPd catalysts can be seen in Fig. 1 with the enhanced activity of the 0.5% Au–0.5% Pd/TiO$_2$ catalyst clear over the course of a 1 h reaction, with concentrations of H$_2$O$_2$ (0.30 wt.%) near double that produced over the 0.25% Au–0.25% Pd/TiO$_2$ catalyst, (0.17 wt.%) which in turn is near double that produced over the 0.125% Au–0.125% Pd/TiO$_2$ analogue (0.08 wt.%). The enhanced activity of the 0.5% Au–0.5% Pd/TiO$_2$ catalyst
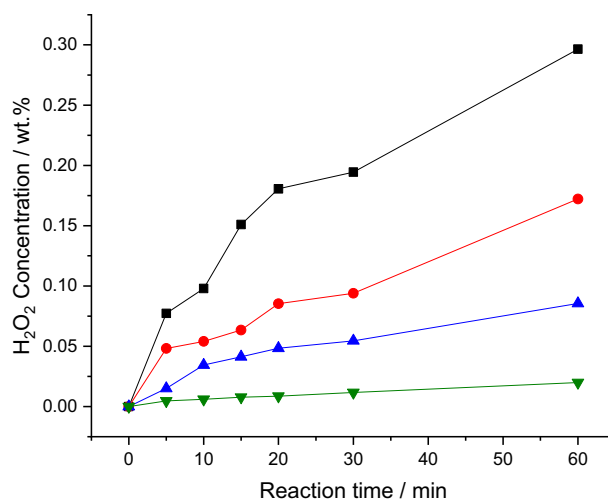

Fig. 1 Comparison of catalytic activity towards H$_2$O$_2$ synthesis as a function of reaction time. H$_2$O$_2$ direct synthesis reaction conditions: Catalyst (0.01 g), H$_2$O (2.9 g), MeOH (5.6 g), 5% H$_2$/CO$_2$ (420 psi), 25% O$_2$/CO$_2$ (160 psi), 0.5 h, 2 °C 1200 rpm. Key: 0.5% Au–0.5% Pd/TiO$_2$ (Black squares), 0.25% Au–0.25% Pd/TiO$_2$ (Red circles), 0.125% Au–0.125% Pd/TiO$_2$ (Blue triangles), 0.0625%Au–0.0625%Pd/TiO$_2$ (Green inverted triangles)

is also highlighted through comparison of calculated reaction rates at reaction times where there is assumed to be no contribution from subsequent degradation reactions or limitations associated with reactant availability (Table S.2).

Evaluation of catalytic activity over multiple sequential H$_2$O$_2$ synthesis tests, where the reactant gas is replaced at 0.5 h intervals, can be seen in Fig. 2. In keeping with our previous observations, a marked enhancement in H$_2$O$_2$ concentration is observed for the 0.5% Au–0.5% Pd/TiO$_2$ catalyst compared to the remaining AuPd catalysts, with this value increasing to a value of 0.61 wt.% after five consecutive synthesis reactions. It should be noted that concentrations of H$_2$O$_2$ achieved by the 0.5% Au–0.5% Pd/TiO$_2$ catalyst is comparable to that achieved during the initial stages

Table 3 Summary of catalytic testing data for supported AuPd/TiO$_2$ catalysts as a function of total metal loading

Catalyst	Productivity/ mol$_{H2O2}$ kg$_{cat}^{-1}$ h^{-1}	H$_2$O$_2$/wt.%	H$_2$ Con./%	H$_2$O$_2$ Sel./%	Apparent reaction rate at 0.5 h/mmol$_{H2O2}$ mmol$_{metal}^{-1}$ h^{-1}	Degradation/ mol$_{H2O2}$ kg$_{cat}^{-1}$ h^{-1}
0.5% Au–0.5% Pd/TiO$_2$	96	0.19	24.4	53.1	1.24×10^3	227
0.25% Au–0.25% Pd/TiO$_2$	56	0.11	12.4	64.8	1.54×10^3	156
0.125% Au–0.125% Pd/TiO$_2$	29	0.05	8.1	71.0	2.19×10^3	88
0.0625% Au–0.0625% Pd/TiO$_2$	5	0.01	N.D	N.D	3.82×10^2	72
TiO$_2$	0	0	0	0	0	0

H$_2$O$_2$ direct synthesis reaction conditions: Catalyst (0.01 g), H$_2$O (2.9 g), MeOH (5.6 g), 5% H$_2$/CO$_2$ (420 psi), 25% O$_2$/CO$_2$ (160 psi), 0.5 h, 2 °C 1200 rpm. H$_2$O$_2$ degradation reaction conditions: Catalyst (0.01 g), H$_2$O$_2$ (50 wt.% 0.68 g) H$_2$O (2.22 g), MeOH (5.6 g), 5% H$_2$/CO$_2$ (420 psi), 0.5 h, 2 °C 1200 rpm

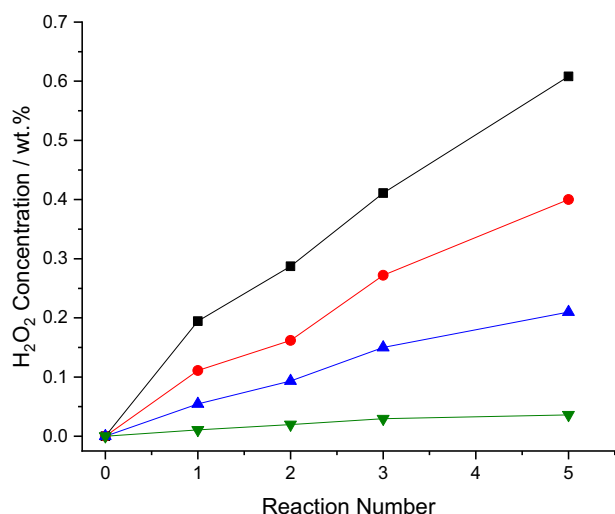*N.D* unable to determine due to detection limits

Fig. 2 Comparison of catalytic activity over sequential H_2O_2 synthesis reactions. H_2O_2 direct synthesis reaction conditions: Catalyst (0.01 g), H_2O (2.9 g), MeOH (5.6 g), 5% H_2/CO_2 (420 psi), 25% O_2/CO_2 (160 psi), 0.5 h, 2 °C 1200 rpm. Key: 0.5% Au–0.5% Pd/TiO$_2$ (Black squares), 0.25% Au–0.25% Pd/TiO$_2$ (Red circles), 0.125%Au–0.125%Pd/TiO$_2$ (Blue triangles), 0.0625% Au–0.0625% Pd/TiO$_2$ (Green inverted triangles)

of the industrial route to H_2O_2 production, prior to the use of multiple distillation steps to raise H_2O_2 concentrations to exceed ~70 wt.% [40].

With the requirement to reuse a catalyst successfully at the heart of green chemistry and the activity of homogeneous species towards H_2O_2 formation well known [41], we next evaluated catalytic activity towards H_2O_2 synthesis and H_2O_2 degradation pathways upon reuse (Table 4). It can be seen that for all catalysts, H_2O_2 synthesis rates decreased significantly, with a corresponding decrease in

initial reaction rate (Table S.2). This loss of catalytic performance upon reuse cannot be ascribed to leaching of metal species, as evidenced from analysis of the H_2O_2 synthesis reaction solution by ICP-MS (Table S.3), which reveals the high stability of the AuPd catalysts during the H_2O_2 synthesis reaction. XPS analysis of the catalysts, as-prepared and after use in the direct synthesis reaction indicates a minor increase in the proportion of Pd^0 as a result of use in the direct synthesis reaction, (Figure S.4), likely as a result of in-situ reduction. While the high activity of Pd^0-rich species towards the degradation of H_2O_2 is well known [42] we cannot ascribe the loss of H_2O_2 synthesis activity observed upon reuse to an increase in competitive H_2O_2 degradation reactions, with this metric comparable in both the initial and second use of these materials in the degradation reaction (Table 4). However, our analysis via XPS does reveal a significant loss in chloride content after use in the direct synthesis reaction, (Figure S.5) with halide ions well known promoters for the direct synthesis reaction it is likely that the loss of Cl is responsible for the observed decrease in catalytic activity towards H_2O_2 formation. Indeed, subsequent studies, where Cl (in the form of $CaCl_2$ or $MgCl_2$) is used in conjunction with a used 0.5% Au–0.5% Pd/TiO$_2$ catalyst leads to a dramatic improvement in H_2O_2 synthesis activity, further highlighting the promotional role of Cl (Figure S.6).

With the observed loss in H_2O_2 synthesis activity upon reuse we were motivated to investigate the effect of heat treatment regime on catalyst reusability, with a focus on the 0.5% Au–0.5% Pd/TiO$_2$ catalyst (Table 5). We have previously demonstrated that AuPd catalysts prepared via

Table 4 Catalyst reusability towards the direct synthesis and subsequent degradation of H_2O_2

Catalyst	Productivity/ $mol_{H2O2}\,kg_{cat}^{-1}\,h^{-1}$		Degradation/ $mol_{H2O2}\,kg_{cat}^{-1}\,h^{-1}$	
	1st use	2nd use	1st use	2nd use
0.5% Au–0.5% Pd/TiO$_2$	96	38	227	249
0.25% Au–0.25% Pd/ TiO$_2$	56	18	156	150
0.125% Au–0.125% Pd/ TiO$_2$	29	11	88	54
0.0625% Au–0.0625%Pd/ Ti O$_2$	5	4	72	5

H_2O_2 direct synthesis reaction conditions: Catalyst (0.01 g), H_2O (2.9 g), MeOH (5.6 g), 5% H_2/CO_2 (420 psi), 25% O_2/CO_2 (160 psi), 0.5 h, 2 °C 1200 rpm. H_2O_2 degradation reaction conditions: Catalyst (0.01 g), H_2O_2 (50 wt.% 0.68 g) H_2O (2.22 g), MeOH (5.6 g), 5% H_2/CO_2 (420 psi), 0.5 h, 2 °C 1200 rpm

Table 5 Reusability of the 0.5% Au–0.5% Pd/TiO$_2$ catalyst towards the direct synthesis and subsequent degradation of H_2O_2, as a function of heat treatment regime

Heat treatment	Productivity/ $mol_{H2O2}\,kg_{cat}^{-1}\,h^{-1}$		Degradation/ $mol_{H2O2}\,kg_{cat}^{-1}\,h^{-1}$	
	1st use	2nd use	1st use	2nd use
Reduction (4 h 400 °C, 5% H_2/Ar)	96	38	227	249
Calcination (4 h 400 °C, air)	71	40	123	200
Calcination (4 h 400 °C, air) + Reduction (2 h 200 °C, 5% H_2/Ar)	64	42	84	173
Calcination (4 h 400 °C, air) + Reduction (2 h 200 °C, 5% H_2/Ar)	67	47	100	221

H_2O_2 direct synthesis reaction conditions: Catalyst (0.01 g), H_2O (2.9 g), MeOH (5.6 g), 5% H_2/CO_2 (420 psi), 25% O_2/CO_2 (160 psi), 0.5 h, 2 °C 1200 rpm. H_2O_2 degradation reaction conditions: Catalyst (0.01 g), H_2O_2 (50 wt.% 0.68 g) H_2O (2.22 g), MeOH (5.6 g), 5% H_2/CO_2 (420 psi), 0.5 h, 2 °C 1200 rpm

a conventional wet co-impregnation procedure and exposed to an oxidative heat treatment are stable over multiple uses [43]. With this in mind the as-prepared 0.5% Au–0.5% Pd/TiO$_2$ catalyst was first subjected to calcination (4 h, 400 °C, flowing air) followed by a reductive heat treatment (2 h, 200–400 °C, 5%H$_2$/Ar).

It can be seen that exposure of the 0.5% Au–0.5% Pd/TiO$_2$ catalyst to calcination only or calcination followed by reduction results in a decreased activity toward both the direct synthesis of H$_2$O$_2$ and its subsequent degradation in comparison to the reduced only analogue. However, in a similar manner to the 0.5% Au–0.5% Pd/TiO$_2$ catalyst exposed to a reductive heat treatment only, all catalysts show a loss in H$_2$O$_2$ synthesis activity upon reuse. Interestingly the H$_2$O$_2$ degradation rates of the catalysts exposed to a calcination, either as a single heat treatment or as part of a two-stage process increase significantly upon reuse, while the rise in H$_2$O$_2$ degradation of the reduced only sample is comparatively negligible.

Analysis of post reaction solutions via ICP-MS reveals that, unlike in the case of the 0.5% Au–0.5% Pd/TiO$_2$ catalyst exposed to a reductive heat treatment (4 h, 400° C, 5% H$_2$/Ar) alone, exposure to either calcination alone or calcination followed by low temperature reduction (2 h, 200° C, 5% H$_2$/Ar) does result in a small amount of precious metal leaching, indicating the clear benefit of high temperature reduction on catalyst stability (Table S.4). While the loss of precious metal species, in addition to the decrease in catalytic selectivity, as indicated by increased rates of H$_2$O$_2$ degradation, could be responsible for the observed decrease in catalyst performance for the samples exposed to calcination or calcination followed by low temperature reduction, the stability of the sample exposed to high temperature reduction alone indicates an alternative route to deactivation.

Further analysis of the catalysts exposed to a range of heat treatment regimens via XPS (Figure S.7) establishes that Pd exists as both Pd^0 and Pd^{2+}, regardless of heat treatment regime, perhaps unsurprisingly with the exception of the calcined only sample, where Pd exists entirely as Pd^{2+}. In all cases a mixed Pd oxidation state is observed upon reuse, with a slightly increased proportion of Pd^0 observed in those samples which displayed mixed states in the as-prepared materials. As previously observed for the 0.5% Au–0.5% Pd/TiO$_2$ catalyst exposed to a reductive heat treatment alone, there is a significant loss of surface Cl content upon use in the direct synthesis reaction for all catalysts (Figure S.8) and it is this which we consider to be the fundamental cause for the loss in catalytic performance observed upon reuse.

4 Conclusion

The ability of Au incorporation to improve catalytic activity towards the direct synthesis of H$_2$O$_2$ is demonstrated, with the synergistic effects observed when Au and Pd are combined in a 1:1 ratio (wt./wt.) attributed to the development of Pd domains of mixed oxidation state and increased control of nanoparticle size, compared to Au- or Pd-rich analogues. Building on these findings we subsequently established a direct correlation between the total metal loading of supported AuPd catalysts with catalytic activity towards both H$_2$O$_2$ synthesis and its subsequent degradation. Catalytic activity towards H$_2$O$_2$ synthesis is observed to decrease significantly upon reuse, with this loss in catalytic performance ascribed to the loss of Cl, a known promoter for catalytic activity towards H$_2$O$_2$ production.

Declarations

References

1. Lewis RJ, Hutchings GJ (2019) Recent advances in the direct synthesis of H$_2$O$_2$. ChemCatChem 11:298–308
2. Campos-Martin JM, Blanco-Brieva G, Fierro JL (2006) Hydrogen peroxide synthesis: an outlook beyond the anthraquinone process. Angew Chem Int Ed 45:6962–6984
3. Edwards JK, Freakley SJ, Lewis RJ, Pritchard JC, Hutchings GJ (2015) Advances in the direct synthesis of hydrogen peroxide from hydrogen and oxygen. Catal Today 248:3–9
4. Wegner P (2003) Hydrogen peroxide stabilizer and resulting product and applications US20050065052A15
5. Edwards JK, Solsona B, Landon P, Carley AF, Herzing A, Watanabe M, Kiely CJ, Hutchings GJ (2005) Direct synthesis of

hydrogen peroxide from H_2 and O_2 using Au–Pd/Fe_2O_3 catalysts. J Mater Chem 15:4595–4600

6. Blaser B, Worms K, Schiefer J (1964) Stabilizing agent for per-oxy-compunds and their solutions US3122417A

7. Lewis RJ, Edwards JK, Freakley SJ, Hutchings GJ (2017) Solid acid additives as recoverable promoters for the direct synthesis of hydrogen peroxide. Ind Eng Chem Res 56:13287–13293

8. Seo M, Kim HJ, Han SS, Lee KY (2017) Direct synthesis of hydrogen peroxide from hydrogen and oxygen using tailored Pd nanocatalysts: a review of recent findings. Catal Surv Asia 21:1–12

9. Flaherty DW (2018) Direct synthesis of H_2O_2 from H_2 and O_2 on Pd catalysts: current understanding, outstanding questions, and research needs. ACS Catal 8:1520–1527

10. Tian P, Ouyang L, Xu X, Ao C, Xu X, Si R, Shen X, Lin M, Xu J, Han Y (2017) The origin of palladium particle size effects in the direct synthesis of H_2O_2: is smaller better? J Catal 349:30–40

11. Kim S, Lee D, Lee K, Cho E (2014) Effect of Pd particle size on the direct synthesis of hydrogen peroxide from hydrogen and oxygen over Pd core-porous SiO_2 shell catalysts. Catal Lett 144:905–911

12. Arrigo R, Schuster ME, Abate S, Wrabetz S, Amakawa K, Teschner D, Freni M, Centi G, Perathoner S, Hävecker M, Schlögl R (2014) Dynamics of palladium on nanocarbon in the direct synthesis of H_2O_2. Chemsuschem 7:179–194

13. Wilson NM, Flaherty DW (2016) Mechanism for the direct synthesis of H_2O_2 on Pd clusters: heterolytic reaction pathways at the liquid–solid interface. J Am Chem Soc 138:574–586

14. Adams JS, Chemburkar A, Priyadarshini P, Ricciardulli T, Lu Y, Maliekkal V, Sampath A, Winikoff S, Karim AM, Neurock M, Flaherty DW (2021) Solvent molecules form surface redox mediators in situ and cocatalyze O_2 reduction on Pd. Science 371:626–632

15. Freakley SJ, He Q, Harrhy JH, Lu L, Crole DA, Morgan DJ, Ntainjua EN, Edwards JK, Carley AF, Borisevich AY, Kiely CJ, Hutchings GJ (2016) Palladium-tin catalysts for the direct synthesis of H_2O_2 with high selectivity. Science 351:965–968

16. Crole DA, Underhill R, Edwards JK, Shaw G, Freakley SJ, Hutchings GJ, Lewis RJ (2020) The direct synthesis of hydrogen peroxide from H_2 and O_2 using Pd–Ni/TiO_2 catalysts. Phil Trans R Soc 378:20200062

17. Quon S, Jo DY, Han GH, Han SS, Seo M, Lee K (2018) Role of Pt atoms on Pd(1 1 1) surface in the direct synthesis of hydrogen peroxide: nano-catalytic experiments and DFT calculations. J Catal 368:237–247

18. Han G, Xiao X, Hong J, Lee K, Park S, Ahn J, Lee K, Yu T (2020) Tailored palladium–platinum nanoconcave cubes as high performance catalysts for the direct synthesis of hydrogen peroxide. ACS Appl Mater Interfaces 12:6328–6335

19. Wang S, Lewis RJ, Doronkin DE, Morgan DJ, Grunwaldt J, Hutchings GJ, Behrens S (2020) The direct synthesis of hydrogen peroxide from H_2 and O_2 using Pd–Ga and Pd–In catalysts. Catal Sci Technol 10:1925–1932

20. Gu J, Wang S, He Z, Han Y, Zhang J (2016) Direct synthesis of hydrogen peroxide from hydrogen and oxygen over activated-carbon-supported Pd–Ag alloy catalysts. Catal Sci Technol 6:809–817

21. Wang S, Gao K, Li W, Zhang J (2017) Effect of Zn addition on the direct synthesis of hydrogen peroxide over supported palladium catalysts. Appl Catal A 531:89–95

22. Cao K, Yang H, Bai S, Xu Y, Yang C, Wu Y, Xie M, Cheng T, Shao Q, Huang X (2021) Efficient direct H_2O_2 synthesis enabled by PdPb nanorings via inhibiting the O–O bond cleavage in O_2 and H_2O_2. ACS Catal 11:1106–1118

23. Crombie CM, Lewis RJ, Kovačič D, Morgan DJ, Slater TJA, Davies TE, Edwards JK, Skjøth-Rasmussen MS, Hutchings GJ (2021) The selective oxidation of cyclohexane via in-situ H2O2 production over supported Pd-based catalysts. Catal Lett. https://doi.org/10.1007/s10562-020-03511-6

24. Crombie CM, Lewis RJ, Taylor RL, Morgan DJ, Davies TE, Folli A, Murphy DM, Edwards JK, Qi J, Jiang H, Kiely CJ, Liu X, Skjøth-Rasmussen MS, Hutchings GJ (2021) Enhanced selective oxidation of benzyl alcohol via in situ H_2O_2 production over supported Pd-based catalysts. ACS Catal 11:2701–2714

25. Lewis RJ, Ueura K, Fukuta Y, Freakley SJ, Kang L, Wang R, He Q, Edwards JK, Yamamoto MDJ, Hutchings GJ (2019) The direct synthesis of H_2O_2 using TS-1 supported catalysts. ChemCatChem 11:1673–1680

26. Kanungo S, van Haandel L, Hensen EJM, Schouten JC, Neira d'Angelo MF (2019) Direct synthesis of H_2O_2 in AuPd coated micro channels: an in-situ X-Ray absorption spectroscopic study. J Catal 370:200–209

27. Menegazzo F, Manzoli M, Signoretto M, Pinna F, Strukul G (2015) H_2O_2 direct synthesis under mild conditions on Pd–Au samples: effect of the morphology and of the composition of the metallic phase. Catal Today 248:18–27

28. Santos A, Lewis RJ, Malta G, Howe AGR, Morgan DJ, Mapton E, Gaskin P, Hutchings GJ (2019) Direct synthesis of hydrogen peroxide over Au–Pd supported nanoparticles under ambient conditions. Ind Eng Chem Res 58:12623–12631

29. Wilson NM, Priyadarshini P, Kunz S, Flaherty DW (2018) Direct synthesis of H_2O_2 on Pd and Au_xPd_1 clusters: understanding the effects of alloying Pd with Au. J Catal 357:163–175

30. Ouyang L, Da G, Tian P, Chen T, Liang G, Xu J, Han Y (2014) Insight into active sites of Pd–Au/TiO_2 catalysts in hydrogen peroxide synthesis directly from H_2 and O_2. J Catal 311:129–136

31. Li J, Ishihara T, Yoshizawa K (2011) Theoretical revisit of the direct synthesis of H_2O_2 on Pd and Au@Pd surfaces: a comprehensive mechanistic study. J Phys Chem C 115:25359–25367

32. Freakley SJ, Kochius S, van Marwijk J, Fenner C, Lewis RJ, Baldenius K, Marais SS, Opperman DJ, Harrison STL, Alcalde M, Smit MS, Hutchings GJ (2019) A chemo-enzymatic oxidation cascade to activate C–H bonds with in situ generated H_2O_2. Nature Commun 10:4178

33. Sankar M, He Q, Morad M, Pritchard J, Freakley SJ, Edwards JK, Taylor SH, Morgan DJ, Carley AF, Knight DW, Kiely CJ, Hutchings GJ (2012) Synthesis of stable ligand-free gold-palladium nanoparticles using a simple excess anion method. ACS Nano 6:6600–6613

34. Edwards JK, Thomas A, Carley AF, Herzing AA, Kiely CJ, Hutchings GJ (2008) Au–Pd supported nanocrystals as catalysts for the direct synthesis of hydrogen peroxide from H_2 and O_2. Green Chem 10:388–394

35. Scofield JH (1976) Hartree–Slater subshell photoionization cross-sections at 1254 and 1487 eV. J Electron Spectrosc Relat Phenom 8:129–137

36. García T, Agouram S, Dejoz A, Sánchez-Royo JF, Torrente-Murciano L, Solsona B (2015) Enhanced H_2O_2 production over Au-rich bimetallic Au–Pd nanoparticles on ordered mesoporous carbons. Catal Today 248:48–57

37. Ouyang L, Tian P, Da G, Xu X, Ao C, Chen T, Si R, Xu J, Han Y (2015) The origin of active sites for direct synthesis of H_2O_2 on Pd/TiO_2 catalysts: interfaces of Pd and PdO domains. J Catal 321:70–80

38. Gong X, Lewis RJ, Zhou S, Morgan DJ, Davies TE, Liu X, Kiely CJ, Zong B, Hutchings GJ (2020) Enhanced catalyst selectivity in the direct synthesis of H_2O_2 through Pt incorporation into TiO_2 supported AuPd catalysts. Catal Sci Technol 10:4635–4644

39. Wang F, Xia C, de Visser SP, Wang Y (2019) How does the oxidation state of palladium surfaces affect the reactivity and selectivity of direct synthesis of hydrogen peroxide from hydrogen

and oxygen gases? A density functional Study. J Am Chem Soc 141:901–910

40. Li H, Zheng B, Pan Z, Zong B, Qiao M (2018) Advances in the slurry reactor technology of the anthraquinone process for H$_2$O$_2$ production. Front Chem Sci Eng 12:124–131

41. Lunsford JH (2003) The direct formation of H$_2$O$_2$ from H$_2$ and O$_2$ over palladium catalysts. J Catal 216:455–460

42. Choudhary VR, Gaikwad AG, Sansare SD (2002) Activation of supported Pd metal catalysts for selective oxidation of hydrogen to hydrogen peroxide. Catal Lett 83:235–239

43. Edwards JK, Solsona SE, Landon P, Carley AF, Herzing A, Kiely CJ, Hytchings GJ (2005) Direct synthesis of hydrogen peroxide from H$_2$ and O$_2$ using TiO$_2$-supported Au–Pd catalysts. J Catal 236:69–79